Academic Journal of Applied Sciences
ISSN: 3105-0549 (Print), ISSN: 3105-0557 (Online) | Vol. 1, No. 2, 2026

Corrosion Inhibition Performance of Syringaldehyde–1,4-Phenylenediamine Schiff Base on Mild Steel in Different Acidic Media

Yutong Wei, Yue Li *, Yu Zhang, Li Li, Jiawang Shen, Jin Zhou, Chenyi Li, Wanlin Zhu

School of Chemistry and Chemical Engineering, Sichuan Institute of Arts and Science, Dazhou 635000, China

* **Corresponding author**: (Email: 1498418249@qq.com)

Abstract: To investigate the corrosion inhibition performance of syringaldehyde–1,4-phenylenediamine Schiff base on mild steel in different acidic media, syringaldehyde and 1,4-phenylenediamine were used as raw materials to prepare syringaldehyde–1,4-phenylenediamine Schiff base (SPSB), and its structure was characterized by nuclear magnetic resonance. Electrochemical methods (electrochemical impedance spectroscopy and potentiodynamic polarization curves) and the static weight loss method were employed to study the corrosion inhibition behavior of this Schiff base on mild steel in four acidic media (4.44 M HCl, 2.22 M H_2SO_4, 1 M HCl, 0.5 M H_2SO_4) at 25 °C. The results show that, under the same hydrogen ion concentration, the inhibition efficiency of SPSB for mild steel in 4.44 M HCl is higher than that in 2.22 M H_2SO_4, and the inhibition efficiency in 1 M HCl is higher than that in 0.5 M H_2SO_4; within the same acid medium, the inhibition efficiency in high-concentration acid systems is significantly higher than that in low-concentration systems, i.e., the inhibition efficiency in 4.44 M HCl is higher than that in 1 M HCl, and that in 2.22 M H_2SO_4 is higher than that in 0.5 M H_2SO_4.

Keywords: Schiff base, mild steel, acidic medium, corrosion inhibition performance, electrochemical method, weight loss method.

1. Introduction

Metal corrosion is the degradation and deterioration phenomenon of materials caused by the combined action of chemical, electrochemical, and physical factors in environmental media. [1] As a prominent issue in the industrial field, it seriously affects the application of metal materials and the service life of equipment. Mild steel, due to its excellent comprehensive properties and low cost, is widely used in petrochemical, construction, and metal processing industries. However, hydrochloric acid and sulfuric acid are commonly used in industrial production for rust removal and descaling, which easily cause acid corrosion damage to mild steel. Therefore, developing efficient corrosion inhibition methods for mild steel in acidic environments has become a key research focus in the field of corrosion protection [2, 3].

At present, metal corrosion protection mainly includes four methods: material composition modification, surface coating, electrochemical protection, and addition of corrosion inhibitors. Among them, corrosion inhibitors have become the most commonly used method in industry due to their advantages of simple operation, no need for additional equipment, low dosage, and rapid effectiveness [4].

Schiff base compounds are obtained by condensation of amines and aldehydes. Due to the presence of the characteristic imine group (–RC=N–), they can form stable complexes with metal ions. In addition, they have advantages such as low cost, low toxicity, and simple synthesis. Their electron-rich structures can also form adsorption films on metal surfaces, blocking the contact between corrosive media and metals, making them a research hotspot in the field of corrosion inhibitors. They have been widely applied in corrosion inhibition of aluminum, zinc, mild steel, copper, magnesium alloys, and other metals.

In recent years, studies on Schiff base inhibitors have been continuously deepened. Various Schiff bases developed domestically have achieved inhibition efficiencies above 80% in different metals and corrosive media. International studies have clarified the inhibition type and mechanism of Schiff bases for mild steel in acidic environments by combining electrochemical tests and quantum chemical calculations, providing theoretical support for the development of new Schiff base inhibitors [5-7].

With increasing industrial demands for low-carbon, environmentally friendly, and low-cost inhibitors, Schiff bases containing electronegative atoms such as N and O and electron-rich aromatic rings can form stable coordination bonds with metals and exhibit excellent inhibition potential. In this study, syringaldehyde and 1,4-phenylenediamine were used as raw materials to prepare SPSB, and its corrosion inhibition performance on mild steel in hydrochloric acid and sulfuric acid systems with different concentrations was systematically investigated. The effects of acid type and concentration on inhibition performance were clarified, providing experimental basis for the development and industrial application of environmentally friendly Schiff base inhibitors, which is of great practical significance for improving the service life of metal equipment and reducing maintenance costs [6-10].

2. Experimental Section

2.1. Main Chemicals and Instruments

All chemicals used in the experiment were of analytical grade, including syringaldehyde, 1,4-phenylenediamine, methanol, ethanol, hydrochloric acid, sulfuric acid, acetone, and acetonitrile. Syringaldehyde and 1,4-phenylenediamine were produced by Shanghai Titan Technology Co., Ltd.; methanol, ethanol, hydrochloric acid, sulfuric acid, and acetonitrile were produced by Chengdu Kelong Chemical Co.,

Ltd.; acetone was produced by Ningbo Xingfa Chemical Co., Ltd.

The main instruments included a CHI760E electrochemical workstation (Shanghai Chenhua Instrument Co., Ltd.), DF-101S thermostatic water bath (Henan Yuhua Instrument Co., Ltd.), FAI204 analytical balance (Lichen Technology), GX125B infrared drying oven (Tianjin Tester Instrument Co., Ltd.), DZKW-3-8 thermostatic water bath (Beijing Yongguangming Medical Instrument Co., Ltd.), and PS-40A ultrasonic cleaner (Zhejiang Jiugong Automation Co., Ltd.), along with mild steel sheets, volumetric flasks, beakers, graduated cylinders, glass rods, plastic wrap, and droppers.

2.2. Synthesis and Structural Characterization of SPSB

2.2.1. Synthesis Method

Accurately weigh 4.1736 g of syringaldehyde and 1.2388 g of 1,4-phenylenediamine using an analytical balance, and dissolve them completely in ethanol. Transfer the dissolved 1,4-phenylenediamine solution into a constant-pressure dropping funnel, and slowly add it dropwise into a three-neck flask containing the syringaldehyde solution under stirring, with the dropping process controlled within 30 min. Stir and reflux at 25 °C for 4 h. After obvious solid precipitation appears, perform vacuum filtration on the solid–liquid mixture. Wash the filter cake with acetonitrile and dry it in an infrared drying oven to obtain a light-yellow crude product. After purification with acetonitrile, 4.0223 g of SPSB is obtained with a yield of 83.78%. The synthetic route is shown in Figure 1.

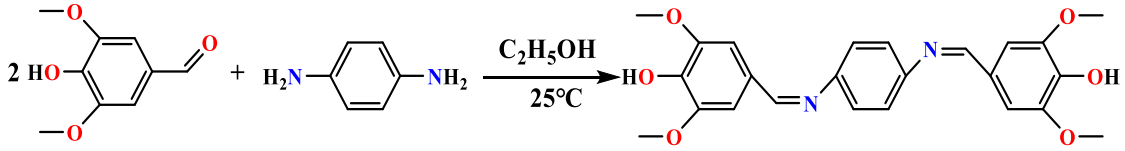

Figure 1. Synthesis route of SPSB Schiff base

2.2.2. Structural Characterization

The molecular structure of SPSB was characterized by ^{1}H NMR (600 MHz, DMSO-d$_6$) (Figure 2): δ 9.15 (s, 2H), 8.53 (s, 2H), 7.27 (d, J = 23.7 Hz, 8H), 3.85 (s, 12H). The signal at δ 9.15 corresponds to –OH protons, 8.53 corresponds to characteristic protons, 7.27 corresponds to aromatic ring protons, and 3.85 corresponds to –CH$_3$ protons. The results confirm that SPSB was successfully synthesized.

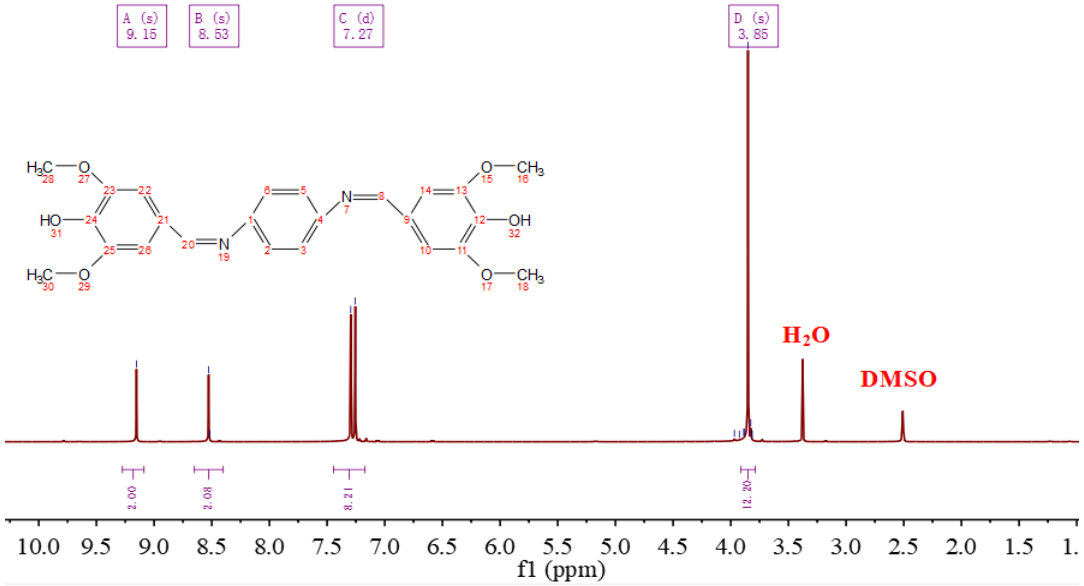

Figure 2. ^{1}H-NMR spectrum of SPSB

2.3. Evaluation Methods of Corrosion Inhibition Performance

2.3.1. Electrochemical Method

In this experiment, a CHI760E electrochemical workstation was used with a standard three-electrode system, where the reference electrode was a saturated calomel electrode, the counter electrode was a platinum electrode, and the working electrode was a cylindrical mild steel electrode with an effective exposed area of 0.196 cm². The corrosion media were four acidic systems: 4.44 M HCl, 2.22 M H_2SO_4, 1 M HCl, and 0.5 M H_2SO_4. The concentrations of the inhibitor SPSB were 0.6, 0.7, 0.8, 0.9, and 1.0 mmol·L^{-1}.

Before electrochemical testing, the electrodes were pretreated by rinsing the reference electrode, platinum electrode, and mild steel electrode with distilled water to keep them clean. The mild steel electrode was manually polished with 1000# sandpaper until the surface became smooth and mirror-like, followed by rinsing with distilled water. The entire electrochemical test was conducted at 25 °C using a thermostatic water bath to reduce random errors.

The testing procedure was as follows: first, open circuit potential (OCP) measurement was carried out with a sampling interval of 0.1 s and a duration of 1200 s to ensure system stabilization; then electrochemical impedance spectroscopy (EIS) measurement was performed with a frequency range of 10^{-2}–10^5 Hz and an amplitude of 5.0 mV, and the experimental data were fitted using ZSimDemo330 software combined with an equivalent circuit (Figure 3) to calculate inhibition efficiency; finally, potentiodynamic polarization

measurement was conducted with a scan range of −0.25 to +0.25 V (relative to OCP) and a scan rate of 5.0 mV·s^{-1}, and the inhibition efficiency was calculated using Tafel extrapolation.

$$\eta_E(\%) = \frac{R'_p - R_P}{R'_P} \times 100\% \quad (1)$$

$$\eta_P(\%) = \frac{I^0_{corr} - I_{corr}}{I^0_{corr}} \times 100\% \quad (2)$$

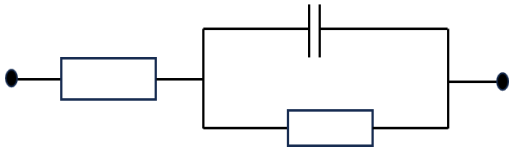

Figure 3. Electrochemical equivalent circuit diagram.

2.3.2. Static Weight Loss Method

The weight loss experiment used mild steel specimens with dimensions of 25 mm × 50 mm × 5 mm. The corrosion media and inhibitor concentrations were consistent with those in the electrochemical method. The experimental temperature was controlled at 25 °C, and three parallel experiments were conducted for each group to reduce random errors.

Sample pretreatment is a key step. Mild steel specimens without deep grooves or scratches were selected and polished sequentially with sandpapers of 60#, 120#, 400#, 800#, 1000#, and 1200# until a bright metallic luster appeared on the surface. The full immersion method was adopted. The pretreated specimens were weighed and recorded (m_1), and their dimensions were measured and labeled. Then, the specimens were immersed in freshly prepared acidic media.

After 4 h, the specimens were removed, washed with distilled water and acetone, and cleaned with an eraser if residues remained on the surface. After drying, the mass (m_2) was measured using an analytical balance. The corrosion rate (v) and inhibition efficiency (η_W) were calculated according to the relevant formulas [11-15].

$$v = \frac{m_1 - m_2}{st} \quad (3)$$

$$\eta_w = \frac{v_0 - v_{inh}}{v_0} \times 100\% \quad (4)$$

Where m_1 and m_2 represent the masses before and after immersion (mg), s is the effective surface area (cm^2), t is the immersion time (h), v_0 is the corrosion rate without inhibitor, and v_inh is the corrosion rate with inhibitor (mg·h^{-1}·cm^{-2}).

3. Results and Discussion

3.1. Electrochemical Impedance Spectroscopy (EIS) Analysis

The impedance data measured by electrochemical impedance spectroscopy were fitted to obtain the solution resistance (R_s) and charge transfer resistance (R_p). T represents temperature, C_{inh} denotes inhibitor concentration, η_E represents inhibition efficiency, CPE represents double-layer capacitance, n denotes the deviation parameter, Y_0 represents the proportionality factor, and χ^2 represents the goodness of fit [16]. The specific electrochemical impedance parameters are listed in Table 1.

From the changes in the Nyquist and Bode plots shown in Figures 4 to 7, it can be observed that in different acidic media at 25 °C, with increasing SPSB concentration, the radius of the capacitive arc increases, indicating an increase in impedance. This suggests that charge transfer is significantly inhibited, implying that a protective film forms on the surface of mild steel, blocking contact between the mild steel and the corrosive medium in the solution. Moreover, the protective film becomes more complete and denser [17], leading to a decrease in corrosion rate and an increase in inhibition efficiency. The Nyquist plot retains a single semicircular structure, indicating that this inhibitor increases the impedance on the mild steel surface without altering the corrosion mechanism. The capacitive arc is not a perfect semicircle, indicating the presence of a frequency dispersion effect during the corrosion process, caused by the non-uniform surface of the mild steel electrode [18]. In the Bode plot, the impedance value increases with increasing inhibitor concentration, indicating that the inhibition efficiency of SPSB for mild steel increases with increasing concentration [19].

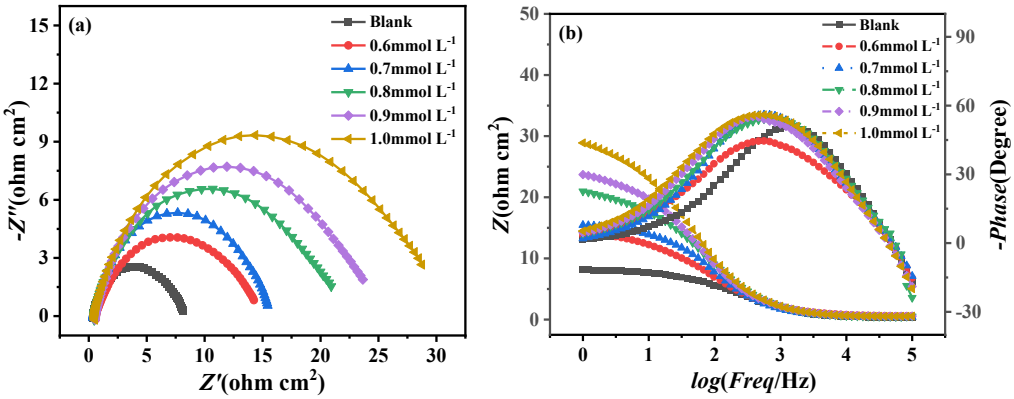

Figure 4. Nyquist and Bode plots of SPSB for mild steel in 4.44 M HCl at 25 °C measured at five different concentrations

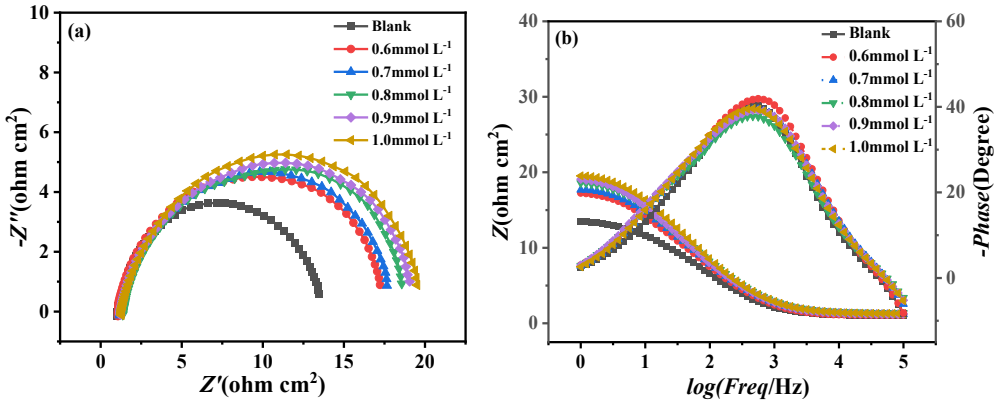

Figure 5. Nyquist and Bode plots of SPSB for mild steel in 2.22 M H_2SO_4 at 25 °C measured at five different concentrations

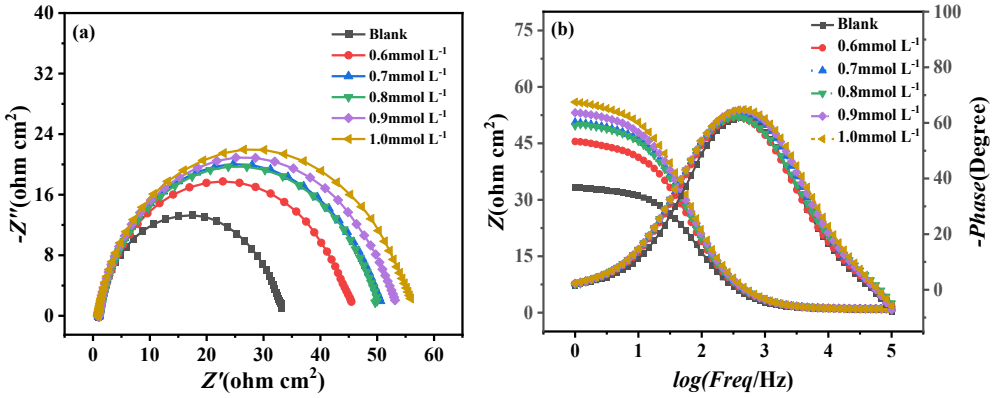

Figure 6. Nyquist and Bode plots of SPSB for mild steel in 1 M HCl at 25 °C measured at five different concentrations

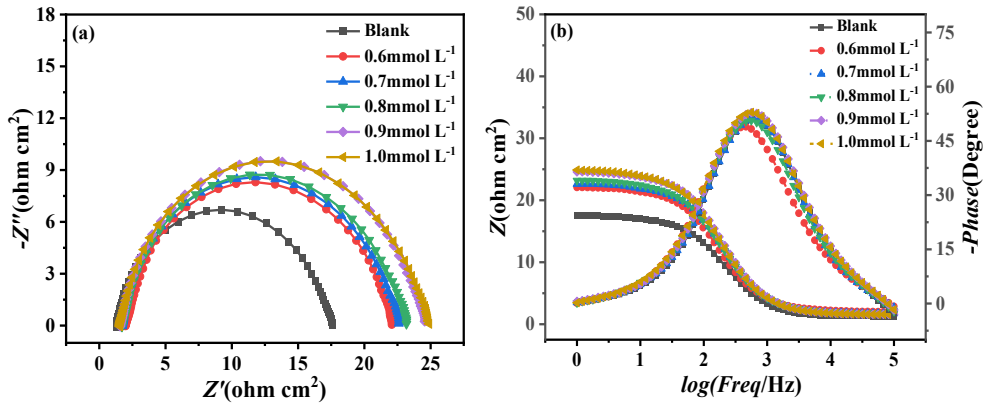

Figure 7. Nyquist and Bode plots of SPSB for mild steel in 0.5 M H_2SO_4 at 25 °C measured at five different concentrations

Table 1. Electrochemical impedance parameters of SPSB for mild steel measured in different acidic media at 25 °C

T (℃)	medium	C_{inh} (mmol L^{-1})	R_s (Ω cm^2)	R_p(Ω cm^2)	n	Y_0 ($\mu\Omega^{-1}$ s^n cm^{-2})	χ^2	η_E (%)
25	4.44M HCl	0	0.3616	7.467	0.8184	438.1	0.0098	/
		0.6	0.5920	13.54	0.7188	1042.0	0.0067	44.85
		0.7	0.3862	14.8	0.8165	501.4	0.0060	49.55
		0.8	0.4533	19.54	0.7893	527.2	0.0129	61.79
		0.9	0.5404	22.74	0.7797	595.5	0.0097	67.16
		1.0	0.5093	27.47	0.7911	524.1	0.0116	72.82
	2.22M H_2SO_4	0	1.0060	12.32	0.7341	1081.0	0.0033	/
		0.6	1.0020	16.03	0.7139	1083.0	0.0054	23.14
		0.7	1.1150	16.75	0.6888	1218.0	0.0031	26.45
		0.8	1.3000	17.59	0.6779	13020.0	0.0028	29.96
		0.9	1.1400	18.11	0.6818	12790.0	0.0035	31.97
		1.0	1.2250	18.54	0.6965	910.0	0.0026	33.55
	1M HCl	0	0.9607	31.86	0.8976	159.6	0.0016	/
		0.6	1.1460	43.77	0.8815	157.9	0.0009	27.21
		0.7	1.0110	48.92	0.8855	141.3	0.0014	34.87
		0.8	1.0870	49.06	0.8665	167.4	0.0010	35.06
		0.9	0.9659	51.42	0.8863	137.7	0.0017	38.04
		1.0	0.9341	54.25	0.8815	134.4	0.0014	41.27
	0.5M H_2SO_4	0	1.3110	16.01	0.8984	138.4	0.0005	/
		0.6	2.0360	20.14	0.8661	163.9	0.0006	20.51
		0.7	1.1710	20.64	0.8953	110.9	0.0002	22.43
		0.8	1.7600	21.30	0.8759	134.7	0.0005	24.84
		0.9	1.6120	22.81	0.8847	115.5	0.0003	29.81
		1.0	1.5760	23.07	0.8812	124.0	0.0004	30.61

As shown in Table 1, upon the addition of SPSB, R_s does not change significantly, while R_p increases with increasing inhibitor concentration in different acidic media. This indicates that as the SPSB concentration increases, the surface coverage of SPSB on the electrode increases, making charge transfer increasingly difficult, thereby improving the inhibition effect. According to the data in the table, the value of n varies little across different acidic media, suggesting that the adsorption of the inhibitor has little effect on the corrosion mechanism. Meanwhile, due to the changes in the surface structure of the electrode, the value of Y_0 varies with the inhibitor concentration. χ^2 represents the goodness of fit; as can be seen from Table 3, the χ^2 values exhibit little variation, indicating that SPSB provides a good fit for mild steel in different acidic media.

From Table 3, under conditions of equal hydrogen ion concentration in the acids, the inhibition efficiency of SPSB for mild steel in 4.44 M HCl is greater than that in 2.22 M H_2SO_4, and the inhibition efficiency in 1 M HCl is greater than that in 0.5 M H_2SO_4. Under the same acid conditions, as the SPSB concentration increases, the inhibition efficiency for mild steel in 4.44 M HCl is greater than that in 1 M HCl, and the inhibition efficiency in 2.22 M H_2SO_4 is greater than that in 0.5 M H_2SO_4. Among these, SPSB exhibits the best inhibition effect on mild steel in 4.44 M HCl, with a maximum inhibition efficiency of 72.82%; the worst inhibition effect is observed in 0.5 M H_2SO_4, with a maximum inhibition efficiency of 30.61%.

3.2. Potentiodynamic Polarization Analysis

The polarization test results of this inhibitor for mild steel in different acidic media are shown in Figures 8 and 9. It can be seen from Figures 8 and 9 that with increasing inhibitor concentration, the corrosion current density significantly decreases in different acidic media, and the inhibition efficiency gradually increases [20]. Compared with the blank solution, the cathodic and anodic polarization curves of mild steel in different acidic media with various concentrations of SPSB all shift negatively. It can also be observed that after the addition of SPSB, both the cathodic and anodic reactions are inhibited to a certain extent.

Table 2 lists the corresponding polarization curve parameters. The relevant electrochemical parameters were obtained using the Tafel extrapolation method, including temperature (T), inhibitor concentration (C_{inh}), inhibition efficiency (η_p), corrosion potential (E_{corr}), corrosion current density (Icorr), anodic Tafel slope (β_a), and cathodic Tafel slope (β_c) [21]. As shown in Table 4, the maximum shift in the corrosion potential (E_{corr}) does not exceed 85 mV, indicating that SPSB is a mixed-type inhibitor [22], capable of inhibiting both anodic dissolution and cathodic hydrogen evolution. The polarization curves of SPSB at different concentrations are nearly parallel to those of the blank solution, suggesting that the addition of SPSB does not fundamentally alter the corrosion mechanism of mild steel, and the inhibition mechanism of SPSB for mild steel follows the "geometric blocking effect" [23]. In different acidic media, as the concentration of SPSB increases, the I_{corr} values continuously decrease, and the inhibition efficiency increases accordingly. This is likely due to the formation of a protective film on the mild steel surface upon the addition of SPSB, which effectively suppresses the corrosion behavior of mild steel in different acidic media. The variation in the inhibition performance of SPSB for mild steel in different acidic media, calculated using Equation (2), is consistent with the EIS results. That is, under conditions of equal hydrogen ion

concentration in the acids, the inhibition efficiency of SPSB for mild steel in 4.44 M HCl is greater than that in 2.22 M H_2SO_4, and the inhibition efficiency in 1 M HCl is greater than that in 0.5 M H_2SO_4. Under the same acid conditions, as the SPSB concentration increases, the inhibition efficiency in 4.44 M HCl is greater than that in 1 M HCl, and the inhibition efficiency in 2.22 M H_2SO_4 is greater than that in 0.5 M H_2SO_4. Among these, SPSB exhibits the best inhibition effect on mild steel in 4.44 M HCl, with a maximum inhibition efficiency of 69.94%, and the worst inhibition effect in 0.5 M H_2SO_4, with a maximum inhibition efficiency of 25.50%.

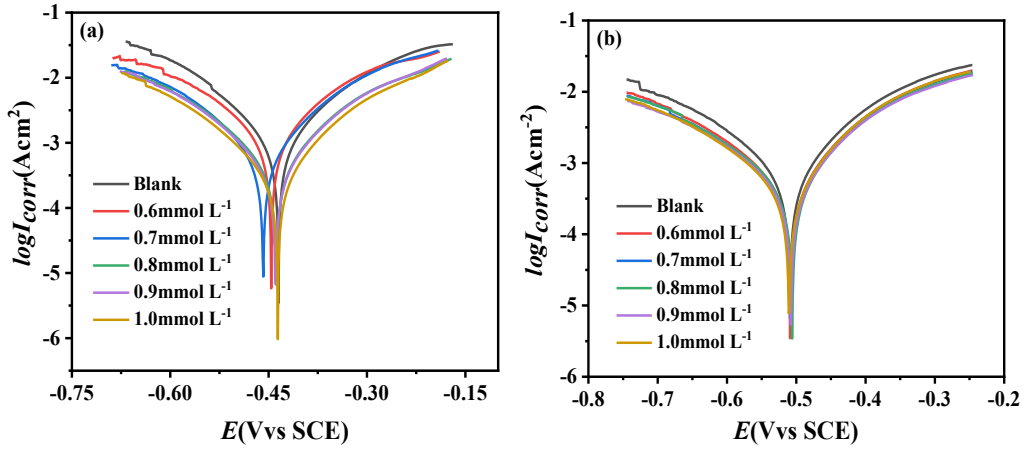

Figure 8. Polarization curves of SPSB for mild steel measured in 4.44 M HCl and 2.22 M H_2SO_4 at 25 °C

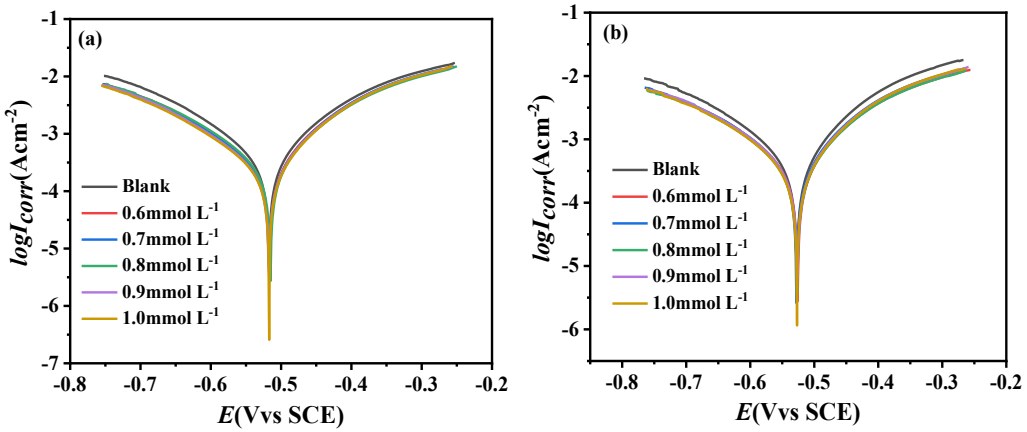

Figure 9. Polarization curves of SPSB for mild steel measured in 1 M HCl and 0.5 M H_2SO_4 at 25 °C

Table 2. Polarization curve parameters of SPSB for mild steel measured in different acidic media at 25 °C

T (°C)	medium	C_{inh} (mmol L^{-1})	I_{corr}(μA cm^{-2})	β_a (mV dec^{-1})	$-\beta_c$ (mV dec^{-1})	E_{corr} (V)	η_p (%)
25	4.44M HCl	0	1088.0	124.66	127.58	-0.435	/
		0.6	1046.0	110.27	121.21	-0.446	38.60
		0.7	656.9	116.29	128.35	-0.458	39.62
		0.8	465.9	117.29	131.60	-0.439	57.18
		0.9	427.9	115.78	132.59	-0.439	60.67
		1.0	327.0	112.37	131.46	-0.436	69.94
	2.22M H_2SO_4	0	758.7	120.58	152.77	-0.509	/
		0.6	541.9	116.44	158.81	-0.509	28.58
		0.7	524.2	114.94	164.42	-0.509	30.91
		0.8	522.3	118.34	173.52	-0.506	31.16
		0.9	500.7	116.95	168.80	-0.508	34.01
		1.0	477.3	112.40	165.62	-0.511	37.09
	1M HCl	0	403.5	116.24	146.26	-0.517	/
		0.6	313.0	112.18	155.18	-0.517	22.43
		0.7	292.7	108.94	152.00	-0.517	27.46
		0.8	286.7	103.34	139.72	-0.515	28.95
		0.9	283.3	109.12	153.44	-0.517	29.79
		1.0	268.8	107.54	156.32	-0.517	33.38
	0.5M H_2SO_4	0	489.4	115.82	160.82	-0.527	/
		0.6	400.5	122.88	164.61	-0.526	18.17
		0.7	388.5	115.75	152.88	-0.528	20.62
		0.8	375.7	121.21	163.11	-0.527	23.23
		0.9	366.5	109.59	149.66	-0.527	25.11
		1.0	364.6	114.26	165.15	-0.528	25.50

3.3. Weight Loss Analysis

Figures 10 and 11 show the weight loss of mild steel caused by SPSB in different acidic media, respectively. The specific weight loss parameters obtained are listed in Tables 5 and 6, where T represents temperature, η_w represents corrosion inhibition efficiency, C_{inh} represents inhibitor concentration, v_{inh} represents corrosion rate, and θ represents surface coverage. This inhibitor has a significant effect on the corrosion rate of mild steel. As the inhibitor concentration increases, the corrosion rate of mild steel gradually decreases. The decrease in the corrosion rate of mild steel is attributed to the adsorption of inhibitor molecules on the surface, forming a protective film that shields the active sites vulnerable to attack by the acidic solution, thereby hindering the corrosion of mild steel by the acidic medium and leading to a gradual increase in inhibition efficiency [24].

From the data in Tables 3 and 4, it can be seen that as the SPSB concentration increases, the corrosion rate of the mild steel specimens gradually decreases, while the inhibition efficiency and surface coverage of SPSB for mild steel in different acidic media both show an increasing trend. It can be deduced that under conditions of equal hydrogen ion concentration in the acids, as the inhibitor concentration increases, the inhibition efficiency of SPSB for mild steel in 4.44 M HCl is greater than that in 2.22 M H_2SO_4, and the inhibition efficiency in 1 M HCl is greater than that in 0.5 M H_2SO_4. Under the same acid conditions, as the inhibitor concentration increases, the inhibition efficiency of SPSB for mild steel in 4.44 M HCl is greater than that in 1 M HCl, and the inhibition efficiency in 2.22 M H_2SO_4 is greater than that in 0.5 M H_2SO_4. Among these, SPSB exhibits the best inhibition effect on mild steel in 4.44 M HCl, with a maximum inhibition efficiency of 76.97%, and the worst inhibition effect in 0.5 M H_2SO_4, with a maximum inhibition efficiency of 30.20%.

A comparison of Tables 1, 2, 3, and 4 shows that this conclusion is consistent with the findings obtained from the electrochemical measurements. The difference between the inhibition efficiencies obtained from the weight loss experiments and those from the electrochemical tests is within 20% [25]. The deviation in inhibition efficiency may be attributed to the limited surface area of the mild steel specimens used in the electrochemical tests, whereas the surface area of the mild steel coupons in the weight loss experiments is larger than that in the electrochemical tests. As the inhibitor concentration increases, the adsorption capacity of the inhibitor on the mild steel surface reaches saturation, which may affect the experimental results [26].

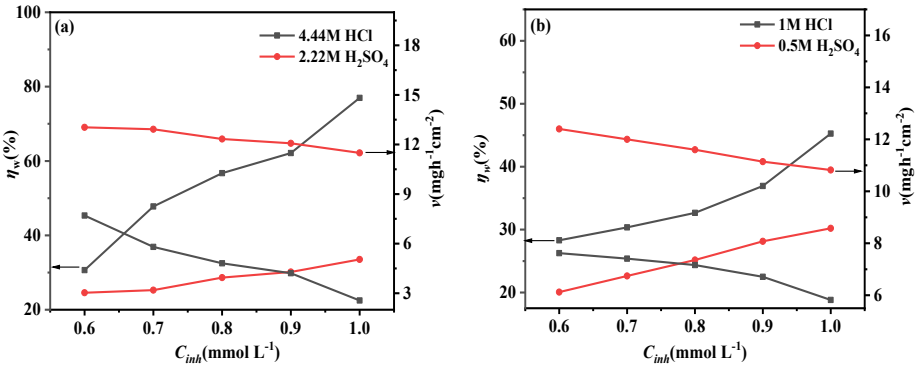

Figure 10. Effect of SPSB on weight loss data of mild steel in different acidic media

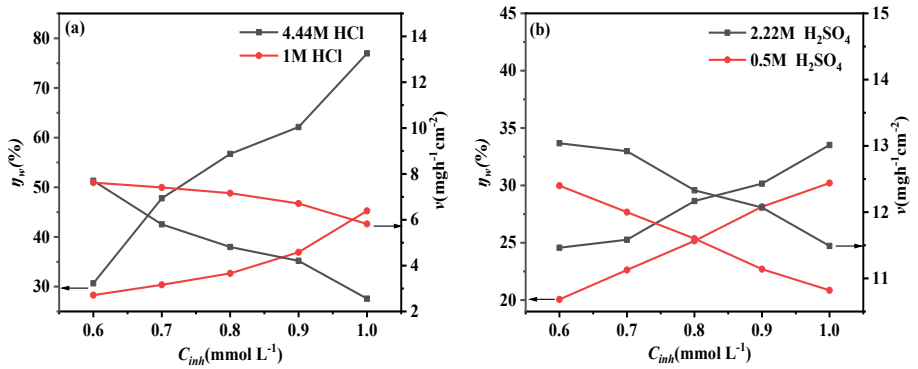

Figure 11. Effect of SPSB on weight loss data of mild steel in different acidic media

Table 3. Weight loss parameters of SPSB for mild steel in 4.44 M HCl and 2.22 M H_2SO_4 at 25 °C

T (°C)	C_{inh} (mmol L^{-1})	4.44M HCl			2.22M H_2SO_4		
		v_{inh}(mg h^{-1} cm^{-2})	η_w (%)	θ	v_{inh}(mg h^{-1} cm^{-2})	η_w (%)	θ
25	0	11.11	/	/	17.28	/	/
	0.6	7.70	30.66	0.3066	13.04	24.57	0.2457
	0.7	5.80	47.78	0.4778	12.92	25.26	0.2526
	0.8	4.81	56.72	0.5672	12.33	28.64	0.2864
	0.9	4.21	62.13	0.6213	12.07	30.15	0.3015
	1.0	2.56	76.97	0.7697	11.49	33.52	0.3352

Table 4. Weight loss parameters of SPSB for mild steel in 1 M HCl and 0.5 M H_2SO_4 at 25 °C

T (°C)	C_{inh} (mmol L^{-1})	1M HCl			0.5M H_2SO_4		
		v_{inh}(mg h^{-1} cm^{-2})	η_w (%)	θ	v_{inh}(mg h^{-1} cm^{-2})	η_w (%)	θ
25	0	10.63	/	/	15.51	/	/
	0.6	7.62	28.30	0.2830	12.40	20.06	0.2006
	0.7	7.41	30.36	0.3036	12.00	22.62	0.2262
	0.8	7.16	32.67	0.3267	11.60	25.16	0.2516
	0.9	6.71	36.93	0.3693	11.14	28.14	0.2814
	1.0	5.82	45.26	0.4526	10.82	30.20	0.3020

4. Conclusions

Syringaldehyde–1,4-phenylenediamine Schiff base (SPSB) was successfully synthesized and confirmed by ^{1}H NMR. Its corrosion inhibition performance on mild steel in four acidic media (4.44 M HCl, 2.22 M H_2SO_4, 1 M HCl, 0.5 M H_2SO_4) at 25°C was systematically studied using electrochemical methods and weight loss measurements, and consistent conclusions were obtained.

At 25°C, the inhibition efficiency of SPSB is significantly affected by acid type and concentration. Under equal hydrogen ion concentration, inhibition efficiency in HCl is higher than in H_2SO_4 (4.44 M HCl > 2.22 M H_2SO_4; 1 M HCl > 0.5 M H_2SO_4). Within the same acid, higher concentration results in better inhibition performance (4.44 M HCl > 1 M HCl; 2.22 M H_2SO_4 > 0.5 M H_2SO_4).

SPSB is a mixed-type inhibitor that acts through adsorption and geometric coverage without changing the corrosion mechanism. The best performance is observed in 4.44 M HCl, with a maximum inhibition efficiency of 76.97% (weight loss method).

This study clarifies the inhibition behavior of SPSB in different acidic media and provides an experimental basis for its industrial application as a corrosion inhibitor for mild steel, as well as a reference for the development and optimization of Schiff base inhibitors.

Acknowledgment

This work was supported by the Sichuan University of Arts and Science Student Innovation and Entrepreneurship Training Program (s202510644115), the Market Supervision Administration of Sichuan Province (SCSJZ2025014), and the Bureau of Science and Technology of Dazhou (24YYJC0003, 2024SSZXDWHZ01).

References

[1] Bai P. W., Meng S. M. Study on corrosion and inhibition performance of mild steel [J]. Sci-Tech Information Development & Economy, 2007 (36): 155-157.

[2] Ding Q. C. Preparation and corrosion inhibition performance of nitrogen-containing polymer corrosion inhibitor [D]. Jishou University, 2019.

[3] Xu S. K. Synthesis and optoelectronic properties of Schiff base-based organic compounds [D]. University of Electronic Science and Technology of China, 2023.

[4] Zhang, W., Li, H. J., Chen, L., et al. Fructan from Polygonatum cyrtonema Hua as an eco-friendly corrosion inhibitor for mild steel in HCl media [J]. Carbohydrate Polymers, 2020, 238, 116216.

[5] Li X. L. Design, synthesis and corrosion inhibition performance of Schiff base corrosion inhibitor for mild steel [D]. Sichuan University of Science & Engineering, 2022.

[6] Li Z. D. Synthesis and corrosion inhibition performance of Schiff base surfactant-type corrosion inhibitor [D]. Hebei University of Technology, 2020.

[7] Xu Y. S. Development and evaluation of aluminum Schiff base corrosion inhibitor in hydrochloric acid medium [D]. Liaoning Normal University, 2021.

[8] Yan L. Y., Ding Y., Li W. Q., et al. Compound vapor phase corrosion inhibitor based on bismorpholinomethyl urea for carbon steel and its inhibition performance [J]. Packaging Engineering, 2023, 44 (17): 276-283.

[9] Wei Z. F., Fu Q. L., Xu L., et al. Study on corrosion inhibition performance of polyurethane surfactant for steel in hydrochloric acid solution [J]. Plating & Finishing, 2024, 46 (02): 37-43.

[10] Qin J. P., Li W. T. Preparation of water-soluble imidazoline corrosion inhibitor from waste cooking oil and its corrosion inhibition performance [J]. Chemical Engineering Design Communications, 2024, 50 (02): 118-120+124.

[11] Wen F. S., Xu Y., Liu W. L. Effect of capric imidazoline quaternary ammonium salt corrosion inhibitor on corrosion inhibition and scale inhibition performance of HEDP system [J]. Corrosion & Protection, 2024, 45 (01): 26-33.

[12] Du W., Yi Z. Y., Xiang R. H., et al. Corrosion inhibition of eucalyptus oil on brass in 5% oxalic acid medium [J]. Electroplating & Finishing, 2023, 42 (14): 64-70.

[13] Ji, K., Jia, W., He, G., et al. Rheological behavior of hydrophobic association polyacrylamides with high salt resistance and corrosion inhibition: Cross-linking modification based on trace dopamine hydrochloride derivatives [J]. Journal of Molecular Liquids, 2024, 400.

[14] Mabrouk, H. D., Morsy, E. E. F., Alsam, A. A. Electrochemical studies, adsorption behavior, and spectroscopic analysis of vanadyl complex of bis(1-(pyridin-2-yl) ethylidene) malonohydrazide as efficient eco-friendly corrosion inhibitor for low carbon steel in 1M HCl [J]. International Journal of Electrochemical Science, 2024, 19 (5).

[15] Chen S. G., Huang X. Y., Li B. Y., et al. Corrosion inhibition performance of cocamidopropyl betaine on carbon steel in sulfuric acid solution [C]//Corrosion Inhibitor Professional Committee of Chinese Society for Corrosion and Protection. Proceedings of the 22nd National Symposium on Corrosion Inhibitors and Water Treatment. [Publisher unknown], 2022: 7.

[16] Dong H. M., Li B. Y., Ran B. Y., et al. Corrosion inhibition mechanism of an eco-friendly corrosion inhibitor linagliptin on copper in sulfuric acid [J]. Journal of Chinese Society for Corrosion and Protection, 2023, 43 (05): 1031-1040.

[17] Wang P. J., Song Y. H., Fan L., et al. Inhibition effect of a novel high-efficiency imidazole Schiff base inhibitor on Q235 steel in 1 mol/L HCl solution [J]. Journal of Chinese Society for Corrosion and Protection, 2024, 44 (01): 59-70.

[18] Xu S. Y. Study on corrosion inhibition performance of N- and S-containing heterocyclic organic compounds for mild steel in acidic media [D]. Chongqing University, 2021.

[19] Zhou L. X., Zhang L. P., Tang Y., et al. Preparation of zinc phytate and its effect on corrosion behavior of Q235 steel [J]. Journal of Chinese Society for Corrosion and Protection, 2024, 44 (02): 396-404.

[20] Liu X. H., Guan J. X., Fu Z. D., et al. Corrosion inhibition performance and mechanism of orange peel extract in H_3PO_4 solution [J]. Surface Technology, 2023, 52 (08): 263-277.

[21] Wang H., Liu J. Q., Tao A. N., et al. Study on corrosion inhibition performance of tea residue extract on Q235 steel in HCl [J]. Journal of Zunyi Normal University, 2023, 25 (05): 96-99.

[22] Chen J. Q., Zhao W. Y., Yao R. C., et al. Synthesis of pistachio shell-based carbon dots and their corrosion inhibition behavior on Q235 carbon steel [J]. CIESC Journal, 2023, 74 (08): 3446-3456.

[23] Liu Y., Xu N. B., Liang S. M., et al. Corrosion inhibition performance of watercress extract in acidic media [J]. Materials Protection, 2019, 52 (04): 33-37.

[24] Shi X. L., Wang J. X., Gao M., et al. Corrosion inhibition performance of furfural derivatives in hydrochloric acid solution [J]. Chemical Industry and Engineering, 2023, 40 (05): 123-134.

[25] Akbari, A. H. Y., Rostami, M., Sari, G. M., et al. Gallic acid-infused LDH nano-containers: A durable protection against mild steel corrosion in simulated seawater [J]. Journal of Molecular Structure, 2024, 1309.

[26] Akrom, M., Rustad, S., Dipojono, K. H. Development of quantum machine learning to evaluate the corrosion inhibition capability of pyrimidine compounds [J]. Materials Today Communications, 2024, 39.